American Mineraolgist, Volume 61, pages 616–625, 1976

Subsolidus equilibria between pyroxenes in the $CaO–MgO–SiO_2$ system at high pressures and temperatures

TAKESHI MORI AND DAVID H. GREEN

Research School of Earth Sciences
Australian National University, Canberra, Australia 2600

Abstract

The extent of pyroxene solid solutions has been experimentally determined in the $CaO–MgO–SiO_2$ system at 30 kbar and 1500°C. The results show the enstatite and diopside mutual solid solutions and also define the limited solid solutions towards olivine and quartz. Although the enstatite–diopside solvus is wider when olivine rather than quartz is a coexisting phase, the difference does not seriously affect the pyroxene solvus as a geothermometer. Thus, this geothermometer can be used without taking the coexisting phases other than pyroxenes into account.

The study of the enstatite–diopside solvus in the $Mg_2Si_2O_6–CaMgSi_2O_6$ system has been extended above 1500°C at 20 and 30 kbar. These pyroxenes show almost complete solid solution at solidus temperatures. The iron-free pigeonite–diopside solvus which was previously found at 20 kbar and inferred to be stable at 30 kbar did not appear at these pressures. The phase equilibrium data in this paper are combined with those in the literature to make a compilation of the enstatite–diopside solvus over a wide temperature–pressure range.

Some difficulties in use of the pyroxene solvus geothermometer are discussed, taking the garnet lherzolite nodules from Lesotho kimberlites as examples.

Introduction

The past few years have seen much interest in the phase equilibrium studies of pyroxenes (Lindsley *et al.*, 1974a; Warner and Luth, 1974; MacGregor, 1974; Smyth, 1974; Nehru and Wyllie, 1974; Howells and O'Hara, 1975; Mori and Green, 1975; and Chen and Presnall, 1975). We note particularly Howells and O'Hara's (1975) treatment of pyroxenes as solid solutions towards forsterite and quartz. The present study, although a continuation of our earlier work, was in part undertaken to evaluate their suggestions.

The enstatite–diopside solvus has long been used as a geothermometer and applied to temperature estimates of natural rocks. An implicit assumption in using the geothermometer is that pyroxenes had no solid solutions towards forsterite and/or quartz. Thus temperatures have been estimated without taking coexisting phases into account. However, Howells and O'Hara (1975) suggested that pyroxenes have solid solutions towards forsterite and quartz and that these solid solutions greatly affect the degree of mutual solid solution. Since all minerals are solid solutions in a strict sense, it is important whether or not the magnitudes of solid solution towards forsterite and quartz are enough to alter the practical application of the solvus as a geothermometer. In this paper we describe experiments made to define these solution limits.

The second problem treated in this paper is a reexamination of the stability of iron-free pigeonite[1] at high pressures. Kushiro (1969) presented a phase diagram in the system $Mg_2Si_2O_6–CaMgSi_2O_6$ at 20 kbar. Pigeonite was thought to be stable above 1450°C, producing two solvi between enstatite and pigeonite, and pigeonite and diopside. Howells and O'Hara (1975) reexamined this system at the same pressure, and contrary to Kushiro's experiments found homogeneous clinopyroxenes well within the pigeonite–diopside solvus as determined by Kushiro. We have reexamined this system at 20 kbar and obtained

[1] Hereafter, this mineral is called pigeonite for convenience. We use this term for low-calcium clinopyroxene which is distinguished from diopside (high-calcium clinopyroxene) by a solvus between them. This definition is also applicable to iron-bearing pigeonite. Note that if the two minerals have the same crystal structure of $C2/c$, it is not necessary to call them by different names.

results supporting Howells and O'Hara's conclusions.

The third experimental problem discussed in this paper is the enstatite–diopside solvus at temperatures above 1500°C at 20 and 30 kbar. The data are supplementary to those previously obtained at lower temperatures by us (Mori and Green, 1975).

Throughout this paper we use mole percent rather than weight percent in describing pyroxene compositions in terms of their end members. Data referred to from the literature have also been converted to mole percent.

Experimental method and results

All the starting materials used in the experiments were mechanical mixtures of two or three synthetic minerals among diopside ($CaMgSi_2O_6$), clinoenstatite ($Mg_2Si_2O_6$), forsterite (Mg_2SiO_4), and quartz (SiO_2). The mixtures were dried and loaded into Pt capsules. We used a piston-cylinder pressure apparatus (Boyd and England, 1960a), and the furnace assemblage included alumina sleeve and alumina thermocouple-insulator to minimize thermocouple contamination and pyrex glass instead of boron nitride outside the graphite heater. A pressure correction of −10 percent of nominal load pressure, using piston-in technique, was applied. No pressure correction was made to thermometry by $W_{97}Re_3/W_{75}Re_{25}$ thermocouples.

All the run products were analyzed by means of the TPD-electron microprobe. Phases were almost free from inclusions and were large enough to avoid chemical contamination from surrounding minerals: the sizes of crystals were up to 60, 40, 20, and 20 microns for enstatite, diopside, forsterite, and quartz, respectively, except for quartz in trace amount (grain size around 4 microns).

The details of experiments are listed in Table 1. Chemical analyses of the run products are shown in Tables 2 and 3.

The extents of pyroxene solid solutions in the $CaO–MgO–SiO_2$ system

Figure 1 is an isothermal, isobaric diagram of the $Di(CaMgSi_2O_6)$–$Fo(2Mg_2SiO_4)$–$Qz(2SiO_2)$ system which is itself a portion of the $CaO–MgO–SiO_2$ system. Though solid solution fields are much exaggerated and are schematic only, two aspects suggested by Howells and O'Hara (1975) are illustrated: firstly, the diopside limb of the enstatite–diopside solvus is less calcic when pyroxenes are coexisting with forsterite rather than with quartz, and secondly, enstatite–diopside tie lines cross the stoichiometric En–Di join from upper left to lower right.

Among the six runs (2B1-2G in Table 1) made at 30 kbar and 1500°C, two had bulk compositions within the three-phase fields, namely, one in the forsterite–enstatite–diopside field and the other in the quartz–enstatite–diopside field, and the remaining

TABLE 1. Results of experiments in the systems $Di(CaMgSi_2O_6)$–$Fo(2Mg_2SiO_4)$–$Qz(2SiO_2)$ and $En(Mg_2Si_2O_6)$–$Di(CaMgSi_2O_6)$

Run No.	Starting materials	Bulk compositions (mole %)	P (kb)	T (°C)	hrs	Products
2B1	Fo, C-En	$Fo_{63.3}\ Qz_{36.7}$	30	1500	4	Fo, En
2B2	C-En, Qz	$Fo_{27.1}Qz_{72.9}$	30	1500	4	En, Qz
2B3	Di, Qz	$Di_{52.8}\ Qz_{47.2}$	30	1500	4	Di, Qz
2B4	Fo, Di	$Di_{73.0}\ Fo_{27.0}$	30	1500	4	Fo, Di
2F	Fo, C-En, Di	$Di_{29.5}\ Fo_{40.9}\ Qz_{29.6}$	30	1500	20	Fo, En, Di
2G	Qz, C-En, Di	$Di_{30.0}\ FO_{29.3}\ Qz_{40.7}$	30	1500	24	Qz, En, Di
Y1	C-En, Di	$En_{66.8}\ Di_{33.2}$	20	1600	6	Di, Qz (tr)
2A3	C-En, Di	$En_{87.0}\ Di_{13.0}$	20	1600	8	En, Di
Y2*	C-En, Di	$En_{83.1}\ Di_{16.9}$	30	1700	2	En, Di
Y3*	C-En, Di	$En_{83.1}\ Di_{16.9}$	30	1600	4	En, Di
2A4	C-En, Di	$En_{71.5}\ Di_{28.5}$	30	1600	10	En, Di, Qz (tr)

C-En: clinoenstatite, En: enstatite, Di: diopside, Fo: forsterite, Qz: quartz. The minerals in the starting materials are of synthetic end member components and those in the run products are solid solutions.
*: disequilibrium.

TABLE 2. Electron probe analyses of olivine, pyroxenes, and quartz in the system Di–Fo–Qz at 30 kbar and 1500°C

Run No.	2B1		2B2		2B3		2B4	
Phase	En	Fo	En	Qz	Di	Qz	Di	Fo
SiO_2	59.55(63)	42.70(20)	60.05(50)	100.37(17)	55.23(63)	98.7(1.8)	54.95(51)	42.32(30)
MgO	39.98(34)	56.49(13)	39.33(33)	0.41(5)	18.18(31)	0.05(4)	19.35(43)	56.10(17)
CaO	-	-	-	-	25.98(32)	0.28(4)	24.82(57)	0.79(9)
Total	99.53(96)	99.19(12)	99.39(70)	100.78(22)	99.4(1.1)	99.1(1.9)	99.12(71)	99.20(46)
Number of ions (olivine: O=4, pyroxene: O=6, quartz: O=4)								
Si	2.000(3)	1.007(4)	2.016(6)	1.994(1)	2.003(2)	1.996(1)	1.994(5)	1.001(3)
Mg	2.001(5)	1.986(7)	1.968(12)	0.012(1)	0.983(10)	0.002(1)	1.047(23)	1.978(5)
Ca	-	-	-	-	1.010(9)	0.006(1)	0.965(22)	0.020(3)
Molecular percent (Di: $CaMgSi_2O_6$, Fo: $2Mg_2SiO_4$, Qz: $2SiO_2$)								
Di	-	-	-	-	100.8(9)	0.6(1)	96.8(2.3)	4.0(5)
Fo	50.0(2)	98.6(7)	48.8(5)	0.3(1)	-0.7(5)	-0.1(1)	2.1(1.1)	97.8(5)
Qz	50.0(2)	1.4(7)	51.2(5)	99.7(1)	-0.1(5)	99.5(1)	1.2(1.3)	-1.8(5)

Run No.	2F			2G			11*	
Phase	En	Di	Fo	En	Di	Qz	En	Di
SiO_2	59.10	56.57	42.79(40)	59.04	57.38	100.26(18)	60.27	57.60
MgO	37.96	26.46	56.78(43)	37.56	26.66	0.21(6)	37.31	26.94
CaO	2.68	16.13	0.35(2)	2.84	15.51	0.15(5)	2.86	15.15
Total	99.74	99.15	99.92(81)	99.44	99.54	100.61(25)	100.44	99.69
Number of ions								
Si	1.996	1.998	1.003(2)	2.000	2.012	1.995(1)	2.018	2.014
Mg	1.911	1.393	1.985(5)	1.897	1.394	0.006(2)	1.862	1.404
Ca	0.097	0.610	0.009(1)	0.103	0.583	0.003(1)	0.103	0.568
Molecular percent								
Di	9.7	61.1	1.7(1)	10.3	57.9	0.3(1)	10.2	56.4
Fo	45.4	19.6	98.5(5)	44.8	20.2	0.1(1)	43.6	20.8
Qz	44.9	19.3	-0.2(4)	44.8	21.9	99.6(1)	46.2	22.9

The numbers in parentheses represent estimated standard errors (1 sigma) and refer to the last decimal place(s). See text for explanations of the data without standard error. *: referred from the supplemental analytical list to Mori and Green (1975). About 10 analyses were obtained for pyroxenes, and 4 for olivine and quartz in each charge.

four runs were on the edges of the Di–Fo–Qz triangle.

For the analyses in Table 2, synthetic forsterite, clinoenstatite, diopside, and quartz were used as substandards additional to the standards used in routine analysis in our laboratory (Reed and Ware, 1973). Thus, we could locate phase boundaries more precisely and could also lower the background uncer-

TABLE 3. Electron probe analyses of pyroxenes in the En–Di system

Run No.	Y1	2A3		Y2	2A4	
P kb	20	20		30	30	
T °C	1600	1600		1700	1600	
Phase	Di	En	Di	En	En	Di
SiO_2	59.06(50)	59.77(41)	59.28(36)	60.44(35)	60.01(23)	58.90(29)
MgO	32.37(83)	36.80(35)	34.42(36)	37.60(36)	36.98(27)	31.37(22)
CaO	8.77(87)	2.83(4)	5.54(27)	2.95(17)	2.72(23)	9.77(36)
Total	100.19(69)	99.40(73)	99.25(51)	100.99(64)	99.72(35)	100.04(40)
Number of ions (O = 6)						
Si	2.016(3)	2.021(3)	2.023(3)	2.014(3)	2.022(3)	2.019(5)
Mg	1.647(34)	1.755(7)	1.751(14)	1.867(10)	1.858(10)	1.603(11)
Ca	0.321(33)	0.103(2)	0.203(10)	0.105(6)	0.098(9)	0.359(13)
Di mole %	32.6(3.4)	10.48(16)	20.8(1.1)	10.67(66)	10.06(84)	36.6(1.2)

The numbers in parentheses represent estimated standard errors (1 sigma) and refer to the last decimal place(s).

tainties in trace element analyses which were caused by X-ray pulse pile-up problems (MgO in quartz, *cf.* Reed and Ware, 1973) and improve accuracy for low concentrations (*e.g.* CaO in olivine and quartz).

The mean compositions and their standard deviations are listed in Table 2. The compositions of pyroxenes in runs (2F and 2G) within the three-phase fields were not well-clustered: enstatite compositions scattered within 3 mole percent Di, and diopside within 6 mole percent. Because our starting materials were the pure phases, we have chosen the most-reacted compositions, *i.e.* diopside with the lowest Di content and enstatite with the highest Di content. The validity of this procedure was discussed by Mori and Green (1975). Table 2 also lists the most-reacted compositions of pyroxenes in an unmixing run (Run 11 of Mori and Green, 1975, the data are from the supplement prepared for the paper). The run charge is saturated or nearly saturated with quartz, and these data plot within 1.5 mole percent from the run 2G of Table 2.

Figure 2 shows the phase relations in a real scale. Note that molar units of Fo and Qz presented in Figure 2 are twice the conventional formulae, so that En has a formula of $Mg_2Si_2O_6$. As shown in the figure, both enstatite and diopside are solid solutions not only between En and Di, but also form limited solid solutions towards Fo and Qz. Non-stoichiometry of pyroxenes has been experimentally shown or suggested by Kushiro (1972) for diopside, by Onuma and Arima (1975) for protoenstatite, and by Boyd and England (1960b) for enstatite. It is also described from natural rocks (*cf.* Sobolev *et al.*, 1968).

The solvus is wider when pyroxenes are saturated

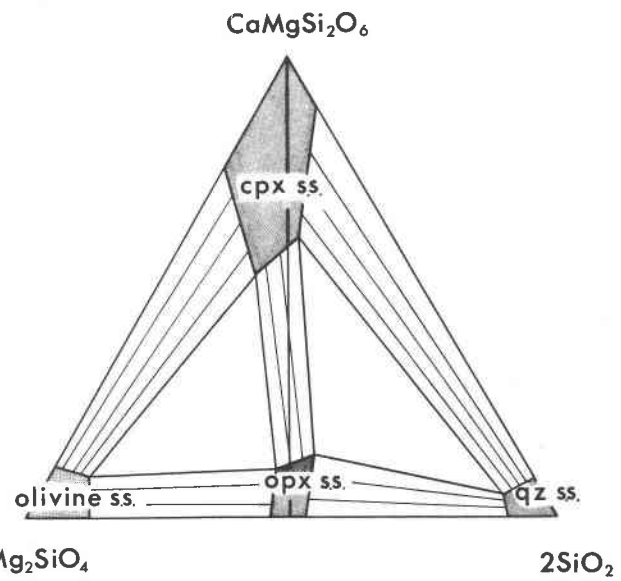

FIG. 1. Isothermal, isobaric phase relations of pyroxenes, olivine, and quartz. Schematic only. See text for explanations.

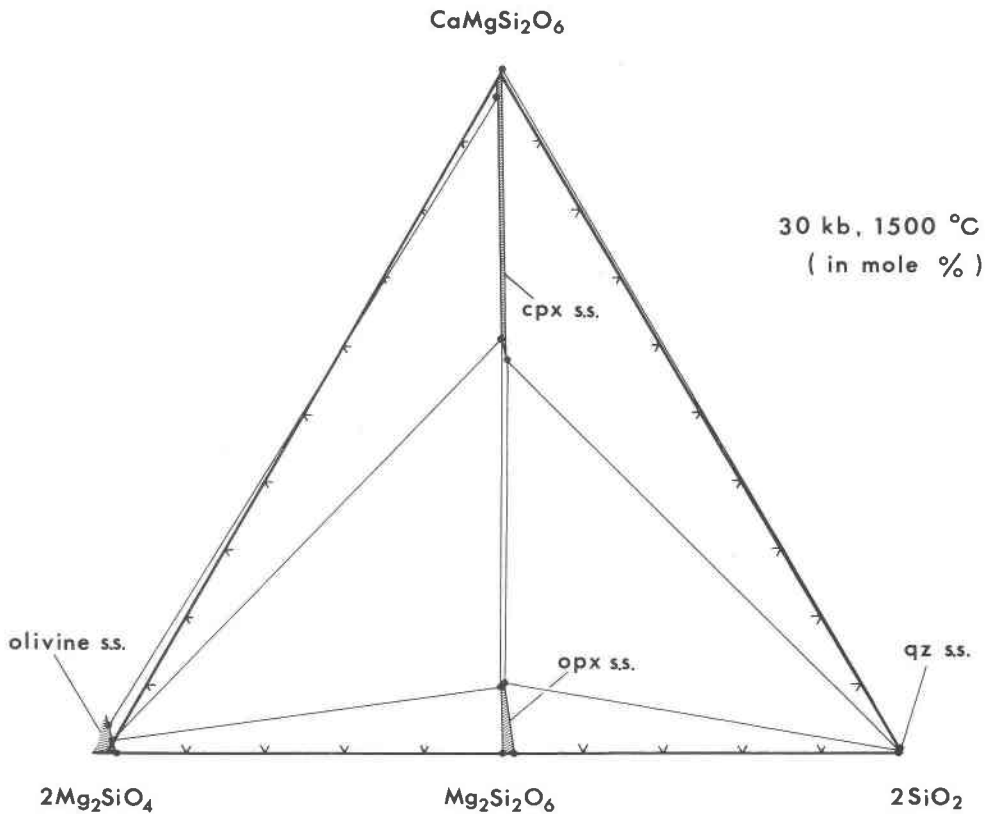

FIG. 2. Experimentally-deduced phase equilibria of olivine, pyroxenes, and quartz at 30 kbar and 1500°C. The hatched areas represent solid solutions. The data (dots) are from Table 2. Note that molar units of forsterite and quartz presented here are twice the conventional formulae.

with forsterite rather than with quartz. This feature is opposite to that inferred by Howells and O'Hara (1975). The difference of the diopside limb in terms of the Di component is about 3 mole percent. This suggests that when the pyroxene solvus is used as a geothermometer at approximately 1500°C and 30 kbar without taking the coexisting phases into account, errors in the temperature estimates of the order of 20°C may result (*cf.* Nehru and Wyllie, 1974; and Mori and Green, 1975). Thus, silica activity does not seriously affect the pyroxene solvus as a geothermometer.

It should also be noted that the enstatite–diopside tie-lines are almost parallel to the En–Di join. The diopside–forsterite tie-line for a charge with a bulk composition on the Di–Fo join clearly crosses the join, in agreement with observations of coexisting natural forsterite and diopside.

Stability of pigeonite–diopside solvus at high pressures in the $Mg_2Si_2O_6$–$CaMgSi_2O_6$ system

Two runs (Y1 and 2A3) at 20 kbar and 1600°C yielded results supporting Howells and O'Hara's (1975) conclusion that there is no stability field of coexisting pigeonite and diopside at this pressure, in contradiction to Kushiro's (1969) phase diagram. The measured compositions of enstatite and diopside grains are shown in Figure 3 and are summarized in Table 3. The synthetic diopside and clinoenstatite loaded into the run Y1 with a bulk composition well within Kushiro's (1969) pigeonite–diopside solvus ($En_{82}Di_{18}$–$En_{50}Di_{50}$) and within Howells and O'Hara's (1975) diopside field homogenized to clinopyroxene although there is some compositional hysteresis. Enstatite was not found in the charge.

The run 2A3 at the same *T-P* conditions had a less calcic bulk composition. Compositions of enstatite and diopside were well clustered with a definition of the diopside limb which coincides with that of Howells and O'Hara (1975) within estimated errors.

Kushiro's (1969) main reason for deducing the presence of a pigeonite–diopside solvus at 20 kbar was the systematic change in intensities of paired 311 X-ray reflections with bulk composition of starting materials. Thus the solvus was located by observing the presence or absence of the paired reflections. For

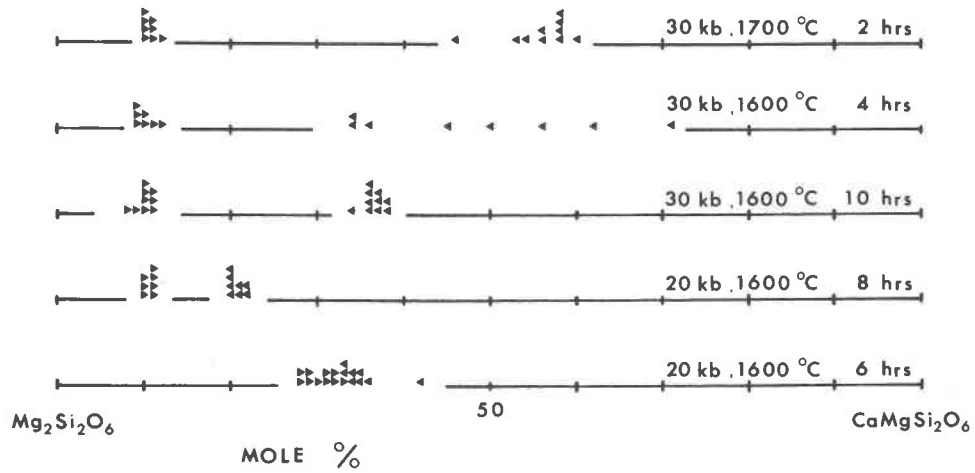

FIG. 3. Microprobe analyses of pyroxenes. All are of homogenization experiments. Direction of triangles shows direction of chemical reaction. Decimal fractions in the raw data have been rounded to the nearest integer.

example, the diopside limb of the solvus at 1600°C and 20 kbar was estimated to be at $En_{50}Di_{50}$.

Alternatively, the 2θ angle of the 311 peak can be more directly used in determining the pyroxene compositions (McCallister, 1974). 2θ values read from Kushiro's Figure 4, combined with McCallister's 2θ-composition equation, which we found very satisfactory, allowed us to estimate the diopside limb of the solvus to be on $En_{28}Di_{72}$, $En_{36}Di_{64}$, or $En_{31}Di_{69}$ at 1600°C and 20 kbar, and on $En_{32}Di_{68}$ at 1650°C and 20 kbar. All the data locate more calcic pyroxenes than the diopside limb as determined by Kushiro at corresponding temperatures. The difference is about 20 mole percent $CaMgSi_2O_6$. In addition, according to Kushiro's Figure 3, liquid, instead of clinopyroxene, is stable for the last composition at 1650°C and 20 kbar. These facts show diffifficulties in the use of paired X-ray reflection to infer the presence or absence of the pigeonite–diopside solvus.

We also cast doubt on the pigeonite–diopside solvus at 17.5 kbar as inferred by Kushiro and Yoder (1970, Fig. 19), which we believe was constructed by an analogy to the solvus at 20 kbar by Kushiro (1969).

Thus, our experiments refute the existence of the pigeonite–diopside solvus at 1600°C and 20 kbar, and the X-ray data of Kushiro (1969), reinterpreted by McCallister's (1974) calibration, can be shown to be inconsistent with the interpretations placed on them by Kushiro (1969). However, there still remains a possibility that a very narrow pigeonite–diopside solvus could exist at 20 kbar and a temperature lower than 1600°C. This possibility is discussed in the next section.

The present state of knowledge is that the pigeonite–diopside solvus is definitely stable only at 1 atmosphere (Yang, 1973; Yang and Foster 1972, and Kushiro 1972), and the maximum pressure for the stability of the solvus remains unknown.

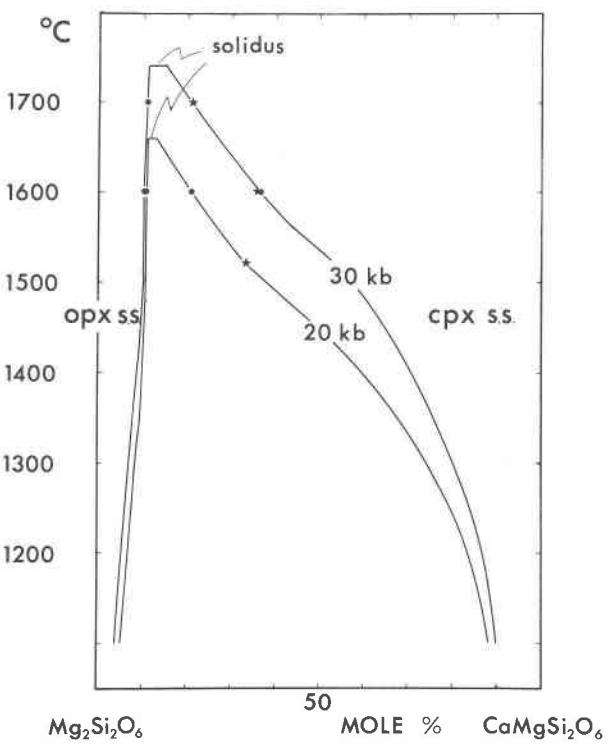

FIG. 4. Comparison of enstatite–diopside solvi at 20 and 30 kbar. Dots are from Table 3, Stars and solidus at 30 kbar are from Howells and O'Hara (1975). The solvi below 1500°C are after Mori and Green (1975). Solidi are only partly drawn. Solidus at 20 kbar is from Kushiro (1969).

Iron-bearing pigeonite has been observed at 15 kbar and 980°C (Lindsley *et al.* 1974b), coexisting with more calcium-rich pyroxene and hypersthene. If pigeonite is unstable in the iron-free system at this pressure, then the pigeonite$_{ss}$–diopside$_{ss}$–hypersthene$_{ss}$ three-phase triangle must converge to a diopside$_{ss}$–hypersthene$_{ss}$ tie-line with decreasing $FeSiO_3$ content (associated with increasing temperature) within the magnesian part of the pyroxene quadrilateral.

The enstatite–diopside solvus in the $Mg_2Si_2O_6$–$CaMgSi_2O_6$ system

Four runs (Y2, Y3, 2A3 and 2A4 in Table 1) at temperatures above 1500°C are relevant to determination of the enstatite–diopside solvus. These are complementary to our previous results at and below 1500°C (Mori and Green, 1975). Again in this study, we experienced sluggishness of chemical reaction, even at temperatures as high as 1700°C. In the runs Y2 (30 kbar and 1700°C) and Y3 (30 kbar and 1600°C), although compositions of enstatite were rather well clustered, those of diopside showed extensive hysteresis in the change in chemistry from the pure diopside ($CaMgSi_2O_6$) of the starting mixes. The run at 30 kbar and 1600°C was repeated with prolonged run duration (10 hours). More closely clustered compositions of diopside resulted. The chemical compositions of pyroxenes in those runs including enstatite of Y2 (30 kbar and 1700°C) are listed in Table 3, and are compared with the data by Howells and O'Hara (1975) in Figure 4. Our data are in good agreement with theirs and further confirm the large pressure effect on the enstatite–diopside solvus at high temperatures.

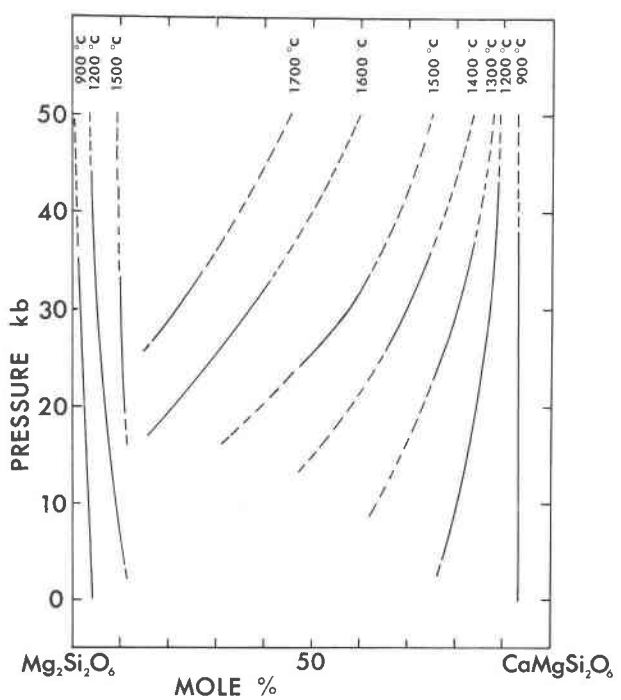

FIG. 5. Compilation of enstatite limbs (the left-side batch of lines) and diopside limbs (the right-side batch of lines) based on the data from Fig. 4 and Mori and Green (1975).

At the solidus between 20–30 kbar, the enstatite and diopside show almost complete solid solution, but melting occurs just below the temperatures at which the enstatite and diopside (with their different crystal structures) limbs would intersect.

A peculiar feature observed in Figure 4 is that the diopside limbs at both 20 and 30 kbar show a slight inflection between 1500 and 1600°C. Although we prefer to regard the figure as an equilibrium phase diagram, there still remains a possibility, as suggested by the presence of the inflection, that the pigeonite–diopside solvus exists around the inflection point at 20 and 30 kbar. In this regard, it is interesting to note that Eggler (1974) suggested a coexistence of two clinopyroxenes at 20 kbar and around 1540°C based on synthesis data in the system CaO–MgO–SiO_2–CO_2. However, the pigeonite–diopside solvus, should it exist at temperatures lower than 1600°C at 20 kbar, must be much narrower than indicated by Kushiro (1969).

The data in Figure 4 were used together with those of Mori and Green (1975) in construction of the pressure-composition section (Fig. 5) which shows enstatite and diopside limbs as a function of temperature and pressure.

Application to temperature and pressure estimates of garnet lherzolite nodules from Lesotho kimberlites, and constraints on the pyroxene-solvus geothermometry

Garnet lherzolite nodules from Lesotho kimberlites have been extensively studied (*e.g.* Boyd, 1973). Physical conditions of equilibration for these nodules can be estimated by solving two independent geothermo-barometers. For this purpose, the MacGregor (1974) and Davis and Boyd's (1966) grids or modifications of them have been commonly used (Boyd, 1973 and Mercier and Carter, 1975).

In this section, we will also try to estimate pressures and temperatures of these nodules using Boyd's extensive chemical data for the minerals of the garnet lherzolite nodules (Boyd, in Nixon, 1973). Although the principle of the method is the same, we will em-

ploy the enstatite–diopside solvus presented in the previous section rather than that of Davis and Boyd (1966). Ca/(Mg + Ca) ratio of diopside from the nodules gives one temperature-pressure equation. Al_2O_3 contents of enstatite coexisting with diopside and garnet and with or without olivine were compiled from the experimental data by Akella and Boyd (1972, 1973, and 1974), Hensen (1973), Mysen and Boettcher (1975), Green (1973), and Mori and Green (unpublished data on the pyrolite system). All the chemical systems include at least SiO_2, TiO_2, Al_2O_3, FeO, MgO, and CaO. Their temperatures and pressures vary from 900 to 1410°C and from 15 to 45 kbar. Consistency among the data is, however, not fully satisfactory. In addition, both geothermo-barometers have to be greatly extrapolated towards higher pressures and temperatures in order to be applied to the garnet lherzolite nodules. These two features greatly limit reliability of this method of temperature–pressure estimates.

Figure 6 shows a graphic method of solving the two equations. Diopside-component isopleths cross the Al_2O_3 (enstatite) isopleths giving unique solutions of temperature and pressure. Boyd's analytical data (Boyd, in Nixon 1973) show that Al_2O_3 content in enstatite is rather constant through the nodules (Al_2O_3 = 1.1 ± 0.3 wt.%), while the Ca/(Mg + Ca) ratio varies extensively from 0.481 to 0.287. This means that the temperature–pressure trend is dependent on the Al_2O_3 isopleths and is linear within ± 3 kbar, which roughly corresponds to the variation of ± 0.3 percent Al_2O_3. If the nodules are classified into granular and sheared types (Boyd, 1973), we can find that the sheared type is more aluminous than the granular type by 0.3 weight percent. The diopside-component isopleths only limit the extent of the temperature–pressure trend determined by the Al_2O_3 isopleths.

A few data points from Boyd (in Nixon, 1973) are plotted in Figure 6. The highest temperature–pressure rock (1597, not plotted in Fig. 6) is estimated at about 85 kbar and 1950°C, and other sheared nodules approach these conditions (Fig. 6). The granular nodules yield temperatures up to 1170°C. Many granular type nodules plot at lower temperatures than 900°C, but the diopside-component isopleths become temperature-insensitive. Thus, the lowest temperature–pressure values cannot be reasonably estimated.

Our estimates are very different from those by Boyd (1973) and Mercier and Carter (1975). The rather narrow range of pressure (up to 70 kbar) and

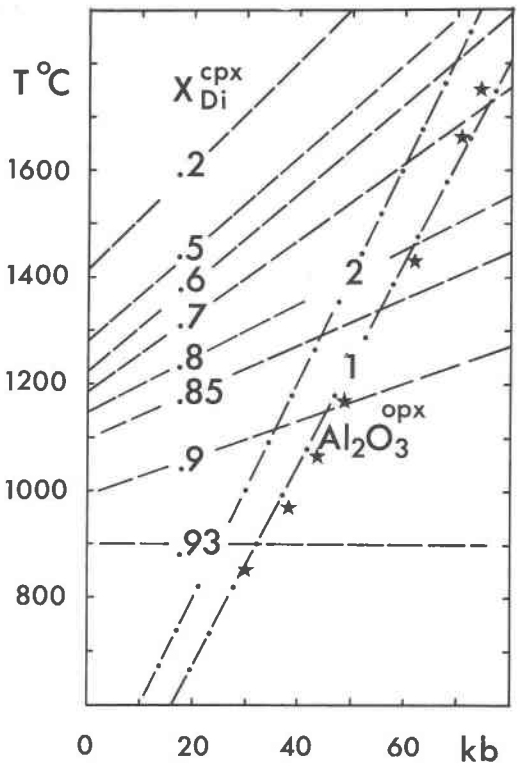

FIG. 6. Method of temperature and pressure estimates. Compositions of diopside limbs (broken lines, in $CaMgSi_2O_6$ mole fraction) are from Mori and Green (1975) and this paper. Al_2O_3 contents in enstatite (lines with dots, in wt. %) are from Akella and Boyd (1972, 1973, and 1974), Hensen (1973), Green (1973), Mysen and Boettcher (1975), and our unpublished data. The stars represent temperature–pressure estimates for garnet lherzolite nodules (1572, 2302A, 1559B, 1859N, 2273, E3, and 1924) from Lesotho kimberlites (Nixon, 1973). In plotting the natural diopsides we have used the ratio 2Ca/(Ca + Mg). Construction of this figure involved large extrapolation of the data and neglect of some inconsistencies among Al_2O_3 data. The deduced *P,T* conditions may be far from the true values (see text).

temperature (up to 1430°C) by Boyd (1973) is mainly due to his use of the enstatite–diopside solvus of Davis and Boyd (1966) at 30 kbar, which shows a more calcic diopside limb below 1000°C and less calcic limb above it compared to our solvus. Mercier and Carter's (1975) revision shows temperature and pressure values up to 80 kbar and 1600°C. Again, the difference from the trend in Figure 6 is mainly due to their scheme for the enstatite–diopside solvus, which has less pressure effect on the solvus than ours.

It might be considered that the temperature–pressure trend in Figure 6 is too steep to repre-

TABLE 4. Accuracy of TPD-probe analysis

	JG-1		JB-1	
	recommended value	TPD-probe	recommended value	TPD-probe
SiO_2	72.95	73.06(41)	53.53	53.64(21)
TiO_2	.26	.26(4)	1.38	1.33(4)
Al_2O_3	14.36	14.42(30)	14.87	14.83(13)
FeO_{total}	1.99	1.89(4)	8.31	8.53(8)
MnO	.06	n.d.	.15	.03(7)
MgO	.75	.99(4)	7.91	7.93(12)
CaO	2.22	2.21(5)	9.50	9.47(7)
Na_2O	3.41	3.25(9)	2.87	2.75(14)
K_2O	4.00	3.93(5)	1.47	1.47(5)

The recommended values for the standard rocks are from Ando et al. (1974). Both sets of data are recalculated to total of 100. The numbers in parentheses represent estimated standard errors (1 sigma) of the probe analysis, and refer to the last decimal place(s).

sent a palaeogeotherm. From present knowledge, we do not know whether the nodule trend is an artifact due to lack of data for phase equilibria at very high pressures and temperatures. In addition, we do not know that the temperature–pressure thus estimated represents a palaeogeotherm.

The principal difficulty in temperature estimates on the basis of the pyroxene solvus is, as shown in the example above, the fact that we have to know pressure values by an independent method. In addition, the solvus is almost useless at temperatures below 900°C. We emphasize that the pressure–temperature estimates of Figure 6 are an *illustration* of the effect that the new solvus data have on the methods of pressure–temperature estimation used by Boyd (1973). We consider that the estimates of pressure–temperature in Figure 6 have very large uncertainties indeed.

Appendix: Accuracy of TPD-microprobe analysis

Standard rocks (JG-1 and JB-1) of Geological Survey of Japan were melted on an iridium strip heater following the melting procedure of Nicholls (1974). The glasses were analyzed by TPD-microprobe using the energy-dispersive analytical system with the routine analytical procedure in our laboratory (Reed and Ware, 1973) but with defocussed beam (about 100 microns). The raw data and the recommended values for the standard rocks (Ando *et al.* 1974) were recalculated to total of 100. This was necessary in order to compare the two sets of data since H_2O^+ and H_2O^- *etc.* evaporate during the melting process.

The results are listed in Table 4. The probe data are satisfactory except for MnO. Concentrations of MnO in these rocks are nearly the same or just above the detection limit of MnO by TPD-probe (about 0.08 wt.%). For those elements with very low concentrations, the conventional wavelength-dispersive microprobe system must be used instead of the energy-dispersive TPD-microprobe. It should be noted that the standard deviations in Table 4 are due almost entirely to heterogeneities of the glasses.

Acknowledgments

We benefitted from discussions with M. Obata (M.I.T.), G. Brey (A.N.U.), I. Kushiro (Geophys. Lab.) and J.R. Smyth (Lunar Science Inst.). Technical assistance by W.O. Hibberson, N.G.

Ware and E.H. Pedersen was particularly helpful. D.H. Eggler (Geophys. Lab.) and A.L. Boettcher (Penn. State Univ.) reviewed the manuscript with constructive criticism. These contributions are gratefully acknowledged.

References

AKELLA, J. AND F. R. BOYD (1972) Partitioning of Ti and Al between pyroxenes, garnets, and oxides. *Carnegie Inst. Wash. Year Book* **71,** 378–384.

——— AND ——— (1973) Effect of pressure on the composition of co-existing pyroxenes and garnet in the system $CaSiO_3$–$MgSiO_3$–$FeSiO_3$–$CaAlTi_2O_6$. *Carnegie Inst. Wash. Year Book,* **72,** 523–526.

——— AND ——— (1974) Petrogenetic grid for garnet periodotites. *Carnegie Inst. Wash. Year Book,* **73,** 269–273.

ANDO, A., H. KURASAWA, T. OHMORI AND E. TAKEDA (1974) 1974 compilation of data on the G.S.J. geochemical reference samples JG-1 granodiorite and JB-1 basalt. *Geochem. J.* **8,** 175–192.

BOYD, F. R. (1973) A pyroxene geotherm. *Geochim. Cosmochim. Acta,* **37,** 2533–2546.

——— AND J. L. ENGLAND (1960a) Apparatus for phase equilibrium measurements at pressures up to 50 kb and temperatures up to 1750°C. *J. Geophys. Res.* **65,** 741–748.

——— AND ——— (1960b) Minerals of the mantle. *Carnegie Inst. Wash. Year Book,* **59,** 47–52.

CHEN, C-H. AND D. C. PRESNALL (1975) The system Mg_2–SiO_4–SiO_2 at pressures up to 25 kilobars. *Am. Mineral.* **60,** 398–406.

DAVIS, B. T. C. AND F. R. BOYD (1966) The join $Mg_2Si_2O_6$–$CaMgSi_2O_6$ at 30 kilobars pressure and its application to pyroxenes from kimberlites. *J. Geophys. Res.* **71,** 3567–3576.

EGGLER, D. H. (1974) Effect of CO_2 on the melting of peridotite. *Carnegie Inst. Wash. Year Book,* **73,** 215–224.

GREEN, D. H. (1973) Conditions of melting of basanite magma from garnet peridotite. *Earth Planet. Sci. Lett.* **17,** 456–465.

HENSEN, B. J. (1973) Pyroxenes and garnets as geothermometers and barometers. *Carnegie Inst. Wash. Year Book,* **72,** 527–534.

HOWELLS, S. AND M. J. O'HARA (1975) Palaeogeotherms and the diopside–enstatite solvus. *Nature,* **254,** 406–408.

KUSHIRO, I. (1969) The system forsterite–diopside–silica with and without water at high pressures. *Am. J. Sci. Schairer Vol.* **267-A,** 269–294.

——— (1972) Determination of liquidus relations in synthetic silicate systems with electron probe analysis: the system forsterite–diopside–silica at 1 atmosphere. *Am. Mineral.* **57,** 1260–1271.

——— AND H. S. YODER, JR. (1970) Stability field of iron-free pigeonite in the system $MgSiO_3$–$CaMgSi_2O_6$. *Carnegie Inst. Wash. Year Book,* **68,** 226–229.

LINDSLEY, D. H., H. E. KING JR. AND A. C. TURNOCK (1974a) Compositions of synthetic augite and hypersthene co-existing at 810°C: application to pyroxenes from lunar highlands rocks. *Geophys. Res. Lett.* **1,** 134–136.

———, ———, ——— AND J. E. GROVER (1974b) Phase relations in the pyroxene quadrilateral at 980°C and 15 kbar. *Geol. Soc. Am. Abstracts with Programs,* **6,** 846.

MACGREGOR, I. D. (1974) The system MgO–Al_2O_3–SiO_2: solubility of Al_2O_3 in enstatite for spinel and garnet peridotite compositions. *Am. Mineral.* **59,** 110–119.

MCCALLISTER, R. H. (1974) The exsolution kinetics of a diopside solid solution having the composition 54.1 mole % $CaMgSi_2O_6$, 45.9 mole % $Mg_2Si_2O_6$. *Carnegie Inst. Wash. Year Book,* **73,** 392–396.

MERCIER, J-C. AND N. L. CARTER (1975) Pyroxene geotherms. *J. Geophys. Res.* **80,** 3349–3362.

MORI, T. AND D. H. GREEN (1975) Pyroxenes in the system $Mg_2Si_2O_6$–$CaMgSi_2O_6$ at high pressure. *Earth Planet. Sci. Lett.* **26,** 277–286.

MYSEN, B. O. AND A. L. BOETTCHER (1975) Melting of a hydrous mantle: II. Geochemistry of crystals and liquids formed by anatexis of mantle peridotite at high pressures and high temperatures as a function of controlled activities of water, hydrogen, and carbon dioxide. *J. Petrol.* **16,** 549–593.

NEHRU, C. E. AND P. J. WYLLIE (1974) Electron microprobe measurement of pyroxenes co-existing with H_2O-undersaturated liquid in the join $CaMgSi_2O_6$–$Mg_2Si_2O_6$–H_2O at 30 kilobars, with applications to geothermometry. *Contrib. Mineral. Petrol.* **48,** 221–228.

NICHOLLS, I. A. (1974) A direct fusion method of preparing silicate rock glasses for energy-dispersive electron microprobe analysis. *Chem. Geol.* **14,** 151–157.

NIXON, P. H. (Ed.) (1973) *Lesotho Kimberlites.* Lesotho National Development Corporation, Maseru, Lesotho. 350 p.

ONUMA, K. AND M. ARIMA (1975) The join $MgSiO_3$–$MgAl_2SiO_6$ and the solubility of Al_2O_3 in enstatite at atmospheric pressure. *J. Japan. Assoc. Mineral. Petrol. Econ. Geol.* **70,** 53–60.

REED, S. J. B. AND N. G. WARE (1973) Quantitative electron microprobe analysis using a lithium drifted silicon detector. *X-ray Spectrometry,* **2,** 69–74.

SMYTH, J. R. (1974) Experimental study on the polymorphism of enstatite. *Am. Mineral.* **59,** 345–352.

SOBOLEV, N. V. JR., I. K. KUZNETSOVA AND N. I. ZYUZIN (1968) The petrology of grospydite xenoliths from the Zagadochnaya kimberlite pipe in Yakutia. *J. Petrol.* **9,** 253–280.

WARNER, R. D. AND W. C. LUTH (1974) The diopside-orthoenstatite two-phase region in the system $CaMgSi_2O_6$–$Mg_2Si_2O_6$. *Am. Mineral.* **59,** 98–109.

YANG, H-Y (1973) Crystallization of iron-free pigeonite in the system anorthite–diopside–enstatite–silica at atmospheric pressure. *Am. J. Sci.* **273,** 488–497.

——— AND W. R. FOSTER (1972) Stability of iron-free pigeonite at atmospheric pressure. *Am. Mineral.* **57,** 1232–1241.